PERGAMON International Journal of Multiphase Flow 27 (2001) 1079–1094

International Journal of Multiphase Flow

www.elsevier.com/locate/ijmulflow

Gas absorption in a moving drop containing suspended solids

A. Muginstein, M. Fichman, C. Gutfinger *

Faculty of Mechanical Engineering, Technion – Israel Institute of Technology, Technion city, 32000 Haifa, Israel

Received 17 August 1999; received in revised form 21 October 2000

Abstract

Absorption of gaseous contaminants into liquid drops is a common method for pollution reduction from waste gases. In several applications, the drops contain suspended solids, which dissolve and enhance gas absorption. Most of the research published on this subject considers the absorption process by neglecting the internal circulation inside the drop. The paper considers the effect of internal circulation on gas absorption in liquid drops. For this aim, a mathematical model based on the Whitman film theory, which also accounts for solid dissolution, chemical reaction and molecular diffusion, is developed. The model indicates that internal circulation cannot be neglected for Peclet numbers higher than 100. Under these conditions, internal circulation enhances the mass transfer as compared to the stagnant drop model. The effect of increasing the solids specific area and solubility becomes less important as the Peclet number increases. Good agreement was found between the present model and experimental data from the literature.

Keywords: Gas absorption; Drops; Mass transfer; Diffusion; Convection; Internal circulation

1. Introduction

Gas absorption into drops containing soluble suspended solids has considerable importance in different industrial applications. Spray towers are the most common devices for flue gas desulfurization (FGD) applications in power stations. In this application, sulfur dioxide, SO_2, and other acidic components such as HCl and HF are absorbed into slurry drops containing limestone ($CaCO_3$) particles. The limestone particles dissolve and provide alkaline species for neutralizing the absorbed acidic components.

Ramachandran and Sharma (1969) formulated a mathematical model for gas absorption into slurry containing soluble particles. In their work they defined the conditions under which the

* Corresponding author. Tel.: +972-4 829 2543; fax: +972-4 832 5537.
E-mail address: gutfinge@tx.technion.ac.il (C. Gutfinger).

0301-9322/01/$ - see front matter
PII: S0301-9322(00)00063-X

absorption and solid dissolution processes may be treated in parallel or series. The suggested formulation considered instantaneous chemical reactions in the *stagnant liquid phase*. The results show an enhancement in absorption rate when solids dissolution takes place together with diffusion of the soluble components inside the slurry.

Bjerle et al. (1972) studied the influence of limestone dissolution on SO_2 absorption into limestone slurry in a laminar-jet scrubber. The results were compared with calculations based on the penetration theory (Danckwerts, 1970) of gas absorption into a quiescent liquid. They concluded that limestone dissolution has no impact on the absorption rate. Those results may be explained by the short contact time between the gas and the slurry in the laminar-jet scrubber.

Uchida et al. (1975) proposed to include the effect of limestone dissolution enhancement near the gas–liquid interface into the Ramachandran and Sharma (1969) model. Their calculations show an enhancement in the absorption rate as compared to that of the Ramachandran and Sharma model.

Justification of this approach could be found in the work of Ukawa et al. (1993) on the dissolution process of limestone particles at different pH levels and particle sizes. Additional evidence for the importance of solids dissolution near the gas–liquid interface can be found in the work of Mehra (1996).

Sada et al. (1977), solved the mass balance equations assuming first-order reactions. Two solutions were obtained, one for the case of constant dissolution rate, and the other for the enhanced dissolution rate, in the gas–liquid interface discussed by Ramachandran and Sharma, and Uchida et al. (1975), respectively. All the solutions were compared with experimental results of CO_2 and SO_2 absorption in a well-stirred vessel containing slaked lime slurry, $Ca(OH)_2$. All the models reported to date assumed that the liquid is stagnant, a fact that caused an underestimation of the mass transfer rate from the gas into the liquid-phase.

In order to take into account the affect of liquid circulation inside the drop, one has to consider the fluid dynamics of these phenomena. Hadamard (1911) and Rybczynski (1911) studied the hydrodynamics of falling spherical drops in axisymmetric creeping flow ($Re \ll 1$). Happel and Brenner (1965) summarized their basic assumptions and solutions.

A comprehensive numerical and experimental study was performed by LeClair et al. (1972) on internal circulation inside pure water drops for $Re < 1000$. Their results show that the creeping flow solution of Hadamard and Rybczynski underestimates the velocity of the liquid near the gas–liquid interface, suggesting a lower internal circulation. Good agreement was found between their numerical solution for drops with diameters below 1 mm and experimental results. The numerical calculations show that when $Re > 400$ the liquid velocity near the gas–liquid interface approaches a constant value.

Watada et al. (1970) and Wellek et al. (1970) obtained numerical solutions for mass transfer with a first-order chemical reaction in spherical drops assuming the Hadamard and Rybczinski creeping flow model. They concluded that the internal circulation does not affect gas absorption for short contact times and high reaction rates.

Brogren and Karlsson (1997) developed a model based on penetration theory, to describe absorption of SO_2 into falling drops containing $CaCO_3$ particles. The model includes both instantaneous and finite rate chemical reactions. The liquid-side mass transfer coefficient was correlated with the degree of internal circulation, for different droplet locations in the spray tower. Based on their calculations, it was concluded that solids dissolution enhances gas absorption only

when the drop internal circulation and the slurry pH are low. Their results are similar to those of Watada et al. (1970) and Wellek et al. (1970), showing that for high chemical reaction rates (high limestone dissolution) internal circulation has a minor effect on absorption.

The majority of research published on gas absorption into drops containing solids assumes no internal circulation, although, there is considerable evidence that internal circulation does exist. This is especially true, during drop formation (Sherwood et al., 1975).

To study the effect of internal circulation on the absorption rate inside drops, we present a mathematical model based on the Whitman film theory (Danckwerts, 1970), which takes into account liquid flow near the gas–liquid interface, solid dissolution, chemical reaction and molecular diffusion.

Although the model was developed for drops, it can also be used to analyze absorption from dispersed bubbles, due to the similarity of the physical conditions at the gas–liquid interface.

2. Mathematical model

2.1. Model description

The present model adds the effect of internal circulation inside the liquid drop to the stagnant liquid model presented by Ramachandran and Sharma (1969). The circulation is accounted for through the creeping flow solution of Hadamard and Rybczynski (Happel and Brenner, 1965).

The model which is based on the Whitman film theory (Danckwerts, 1970) is illustrated in Fig. 1. In this model all the reactions between the dissolved species take place in a thin film on the liquid side of the gas–liquid interface.

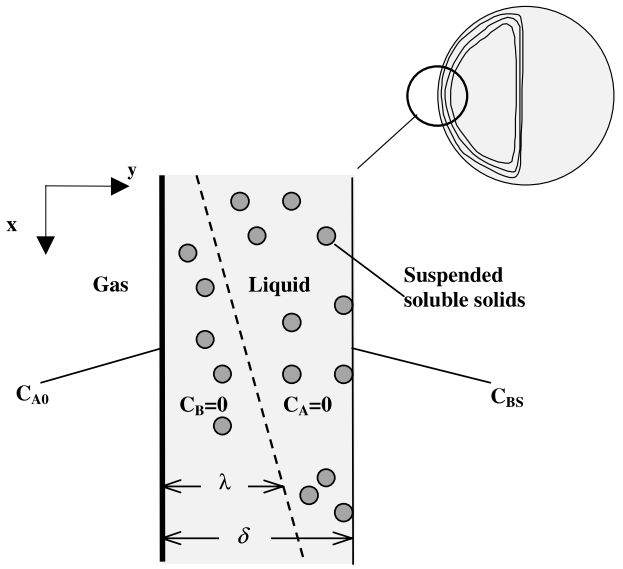

Fig. 1. Mathematical model and boundary conditions.

The figure also shows a magnification of the liquid film, which has a thickness δ. The concentration of the diffusing gas A at the gas–liquid interface – C_{A0} is constant. Inside the drop, outside the liquid film the liquid is saturated with the dissolved solid B at a concentration C_{BS}. The liquid film, in which the reaction takes place, contains suspended particles with diameters much smaller than the thickness of the film.

The dissolved gaseous species A diffuses through the liquid film, and reacts with the dissolved solid species B. The suspended solids in the film dissolve, providing a supply of B that reacts with A, thus enhancing gas absorption and shifting the reaction plane towards the gas–liquid interface.

The problem is formulated under the following assumptions:

(a) The gas-side resistance to mass transfer is negligible, as compared to that of the liquid side.

(b) The chemical reaction in the liquid phase between the dissolved gas A and the dissolved solid B is

$$A + B \rightarrow \text{Product} \tag{1}$$

(c) The reaction is instantaneous, resulting in a thin liquid layer of thickness δ, which develops near the gas–liquid interface. Hence, the problem may be formulated for this layer in a Cartesian system of coordinates.

(d) The solid particles are small and uniformly dispersed throughout the drop, including the thin layer near the gas–liquid interface.

(e) The dissolution near the gas–liquid interface cannot be neglected. The condition for which this assumption is valid is (Ramachandran and Sharma, 1969)

$$\frac{k_s A_p D_A^2}{4 k_l^2 D_B} \ll 1, \tag{2}$$

where A_p is the specific solids area in the slurry, k_s the solids dissolution rate, k_l the liquid mass transfer coefficient in the absence of convection, chemical reaction or solid dissolution and D_A and D_B are the molecular diffusivities of A and B, respectively.

(f) The reactant concentration in the liquid is low, and the viscosity, density and diffusion coefficients are constant.

(g) The velocity in the thin liquid layer near the gas–liquid interface was taken from the classical creeping flow solution of Hadamard (1911) and Rybczynski (1911). For 1–2 mm spherical drops the assumption of creeping flow, $Re \ll 1$, is not justified, and the solution of Hadamard and Rybczynski underestimates the velocity of the liquid near the gas–liquid interface. On the other hand, the solution of LeClair et al. (1972) overestimates the amount of circulation in our case, because it does not accounts for the presence of suspended particles in the drop. The use of the creeping flow solution assures results, which in our opinion are closer to reality.

(h) The velocity in the thin liquid layer near the gas–liquid interface is assumed constant at any cross-section, see Levich (1962, pp. 404,405)

$$v_x = \text{const.} = u. \tag{3}$$

(i) In the present model, the convection velocity, u, is the liquid velocity at the drop equator obtained from the Hadamard and Rybczynski solution. This velocity of the liquid does not change with x within the thin liquid layer. Therefore, from the continuity equation, the velocity in y-direction is zero (LeClair et al., 1972).

(j) For high Peclet numbers, the diffusion boundary layer is very thin compared to the axial dimension (see Levich, 1962, pp. 80,81). Moreover, because of the fast chemical reaction near the gas–liquid interface, the layer that develops near the droplet surface is even thinner. As a result, the diffusion in the x-direction is negligible, compared to that in the y-direction,

$$\frac{\partial^2 C}{\partial y^2} \gg \frac{\partial^2 C}{\partial x^2}. \tag{4}$$

2.2. Mathematical analysis

Taking into account the above assumptions we write the mass balance equations. These equations describe the gas absorption process as one governed by gas diffusion in the liquid on one side, and solid dissolution on the other, in the presence of lateral convection within a thin layer near the drop surface. The rate of reaction between the absorbed gas and the dissolved solid is assumed to be instantaneous. The convection velocity, u, is the lateral liquid velocity at the drop equator obtained from the Hadamard and Rybczynski solution. The mass balance equations and boundary conditions for the absorbed gas A and the dissolved solid B are formulated, respectively, as

$$\begin{aligned} &D_{\mathrm{A}} \frac{\partial^2 C_{\mathrm{A}}}{\partial y^2} - k_{\mathrm{s}} A_{\mathrm{p}} C_{\mathrm{BS}} - u \frac{\partial C_{\mathrm{A}}}{\partial x} = 0, \quad 0 < y < \lambda, \ x > 0, \\ &\text{b.c}: \ C_{\mathrm{A}} = C_{\mathrm{A}i} \quad \text{at } y = 0, \\ &\qquad C_{\mathrm{A}} = 0 \quad \text{at } y = \lambda, \\ &\qquad C_{\mathrm{A}} = 0 \quad \text{at } x = 0, \end{aligned} \tag{5}$$

$$\begin{aligned} &D_{\mathrm{B}} \frac{\partial^2 C_{\mathrm{B}}}{\partial y^2} + k_{\mathrm{s}} A_{\mathrm{p}} (C_{\mathrm{BS}} - C_{\mathrm{B}}) - u \frac{\partial C_{\mathrm{B}}}{\partial x} = 0, \quad \lambda < y < \delta, \ x > 0, \\ &\text{b.c}: \ C_{\mathrm{B}} = C_{\mathrm{BS}} \quad \text{at } y = \delta, \\ &\qquad C_{\mathrm{B}} = 0 \quad \text{at } y = \lambda, \\ &\qquad C_{\mathrm{B}} = C_{\mathrm{BS}} \quad \text{at } x = 0. \end{aligned} \tag{6}$$

The location of the reaction plane is denoted by λ. As the reaction between the absorbed gas and the dissolved solid is instantaneous, hence, the absorbed gas is restricted to the region $0 < y < \lambda$, while the dissolved solid exists only in region $\lambda < y < \delta$.

Eq. (5) for the absorbed gas applies to the region $0 < y < \lambda$. The first term in that equation represents the diffusion rate of the gas. The second term gives the rate of gas disappearance, due to the reaction with the solid, which dissolves at a rate $k_{\mathrm{s}} A_{\mathrm{p}} C_{\mathrm{BS}}$. The third term accounts for the convection of A.

Eq. (6) for the dissolved solid applies to the region $\lambda < y < \delta$. The first term in that equation represents the diffusion rate of the dissolved solid. The second term gives the rate of dissolution of the solid. The third term accounts for convection.To simplify the analysis, the drop is divided into two regions as illustrated in Fig. 2:

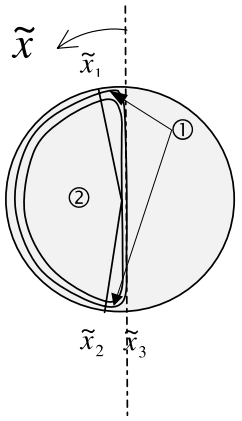

Fig. 2. Regions close to the drop surface where convection is important (2) and where it is not (1).

1. Region 1, where the velocity, and as a result, the convection is negligible.
2. Region 2, where the convection is important. In this region, the liquid velocity is assumed constant.

Eqs. (5) and (6) apply for both regions. In region 2 the velocity u is taken as constant, while in region 1, $u = 0$. The equations were solved independently for each region, without matching at the region boundaries. As region 1 is much smaller than region 2, this simplification is justified (see Appendix A).

We now put the mass balance equations in dimensionless form by defining the following dimensionless quantities:

$$\tilde{x} = \frac{x}{\delta}, \quad \tilde{y} = \frac{y}{\delta}, \quad \xi = \frac{\lambda}{\delta}, \quad \tilde{C}_\mathrm{A} = \frac{C_\mathrm{A}}{C_{\mathrm{A}i}}, \quad \tilde{C}_\mathrm{B} = \frac{C_\mathrm{B}}{C_\mathrm{BS}}, \quad Pe = \frac{u\delta}{D},$$
$$R_\mathrm{A} = \frac{k_\mathrm{s} A_\mathrm{p}}{D_\mathrm{A}} \left(\frac{C_\mathrm{BS}}{C_{\mathrm{A}i}} \right) \delta^2, \quad R_\mathrm{B} = \frac{k_\mathrm{s} A_\mathrm{p}}{D_\mathrm{B}} \delta^2. \tag{7}$$

The mass balance equations now become

$$\frac{\partial^2 \tilde{C}_\mathrm{A}}{\partial \tilde{y}^2} - Pe_\mathrm{A} \frac{\partial \tilde{C}_\mathrm{A}}{\partial \tilde{x}} - R_\mathrm{A} = 0, \quad 0 < \tilde{y} < \xi,$$
$$\text{b.c.} \quad \tilde{C}_\mathrm{A}(x, 0) = 1, \tag{8}$$
$$\tilde{C}_\mathrm{A}(x, \xi) = 0,$$
$$\tilde{C}_\mathrm{A}(0, y) = 0.$$

$$\frac{\partial^2 \tilde{C}_\mathrm{B}}{\partial \tilde{y}^2} - Pe_\mathrm{B} \frac{\partial \tilde{C}_\mathrm{B}}{\partial \tilde{x}} + R_\mathrm{B}(1 - \tilde{C}_\mathrm{B}) = 0, \quad \xi < \tilde{y} < 1,$$
$$\text{b.c.} \quad \tilde{C}_\mathrm{B}(x, 1) = 1, \tag{9}$$
$$\tilde{C}_\mathrm{A}(x, \xi) = 0,$$
$$\tilde{C}_\mathrm{A}(0, y) = 1.$$

In these equations, three dimensionless numbers, the Peclet number, Pe, and the dimensionless reaction rates R_A, R_B characterize the phenomena.

The Peclet number represents the ratio between convection and diffusion and is defined as

$$Pe = \frac{u\delta}{D}, \tag{10}$$

where δ is the thickness of the thin liquid film near the gas–liquid interface, and u, is the lateral velocity of the liquid inside this film. The liquid film thickness δ, has been estimated using the Whitman stagnant film theory (Danckwerts, 1970) as

$$\delta = \frac{D}{k_l}. \tag{11}$$

Here, k_l is the liquid-side mass transfer coefficient in the absence of convection, chemical reaction and solids dissolution, and is used for estimating the liquid film thickness only. Although this coefficient depends generally on the hydrodynamics of the system, its effect is rather small, and may be neglected in the estimate of δ (Handlos and Baron, 1957).

Eqs. (8) and (9) are now solved using eigenfunction expansions (Wyllie, 1995) to yield the dimensionless concentrations of A and B, respectively.

$$C_A(\tilde{x},\tilde{y}) = 1 - \frac{\tilde{y}}{\xi} + \frac{1}{2}R_A\tilde{y}(\tilde{y}-\xi) + \sum_{n=1}^{\infty} D_n \sin\left(\frac{n\pi}{\xi}\tilde{y}\right)\exp\left(-\left(\frac{n\pi}{\xi}\right)^2\frac{\tilde{x}}{Pe}\right), \tag{12}$$

where

$$D_n = \frac{2}{(n\pi)^3}\left[R_A\xi^2(1-(-1)^n) - (n\pi)^2\right],$$

$$C_B(\tilde{x},\tilde{y}) = 1 - \frac{\sinh\left(\sqrt{R_B}(1-\tilde{y})\right)}{\sinh\left(\sqrt{R_B}(1-\xi)\right)} + \sum_{n=1}^{\infty} E_n \sin\left(\left(\frac{n\pi}{1-\xi}\right)(1-\tilde{y})\right) \times \exp\left[-\left(R_B + \left(\frac{n\pi}{1-\xi}\right)^2\right)\frac{\tilde{x}}{Pe}\right], \tag{13}$$

where

$$E_n = \frac{2n\pi(-1)^{n+1}}{R_B(1-\xi)^2 + (n\pi)^2}.$$

Eqs. (12) and (13) provide, respectively, the spatial concentration distribution of species A and B inside the liquid film. Comparing the present two-dimensional solution with that for the one-dimensional model of Ramachandran and Sharma (1969) and Uchida et al. (1975), we note that our solution adds to theirs the x-dependence in the last terms of the right-hand-sides of Eqs. (12) and (13). These two terms account for the circulation inside the drop, expressing the contribution of convection to gas absorption. The effect of circulation becomes more significant for higher Peclet numbers, as can be concluded by viewing the rightmost terms of Eqs. (12) and (13). These

terms approach asymptotically to zero as Peclet number is lowered. Hence, for $Pe \to 0$ Eqs. (12) and (13) simplify to the stagnant film solution of Ramachandran and Sharma (1969),

$$C_{\mathrm{A,stagnant}}(\tilde{x},\tilde{y}) = 1 - \frac{\tilde{y}}{\xi} + \frac{1}{2} R_{\mathrm{A}} \tilde{y}(\tilde{y} - \xi), \tag{14}$$

$$C_{\mathrm{B,stagnant}}(\tilde{x},\tilde{y}) = 1 - \frac{\sinh\left(\sqrt{R_{\mathrm{B}}}(1-\tilde{y})\right)}{\sinh\left(\sqrt{R_{\mathrm{B}}}(1-\xi)\right)}. \tag{15}$$

The location of the reaction plane, $\xi(x)$, is found from the equality of molar fluxes on both sides of the reaction plane.

$$D_{\mathrm{A}} \frac{\partial C_{\mathrm{A}}}{\partial \mathbf{n}}\bigg|_{y=\lambda} = -D_{\mathrm{B}} \frac{\partial C_{\mathrm{B}}}{\partial \mathbf{n}}\bigg|_{y=\lambda}. \tag{16}$$

Eq. (16) is simplified by noting that at low curvature of the reaction plane we may write

$$D_{\mathrm{A}} \frac{\partial C_{\mathrm{A}}}{\partial y}\bigg|_{y=\lambda} = -D_{\mathrm{B}} \frac{\partial C_{\mathrm{B}}}{\partial y}\bigg|_{y=\lambda}. \tag{17}$$

Substitution of the obtained concentrations of A and B into Eq. (17) yields an expression for the dimensionless location $\xi(x)$ of the reaction plane

$$\begin{aligned} &R_{\mathrm{A}} \frac{1}{\xi} - R_{\mathrm{A}}\xi + \frac{D_{\mathrm{B}}}{D_{\mathrm{A}}} \frac{C_{\mathrm{BS}}}{C_{\mathrm{A}i}} \sqrt{R_{\mathrm{B}}} \coth\left(\sqrt{R_{\mathrm{B}}}(1-\xi)\right) \\ &= \sum_{n=1}^{\infty} (-1)^n (n\pi/\xi) D_n \exp\left(-\frac{(n\pi/\xi)^2}{Pe}\tilde{x}\right) + \frac{D_{\mathrm{B}}}{D_{\mathrm{A}}} \frac{C_{\mathrm{BS}}}{C_{\mathrm{A}i}} \left(\sum_{n=1}^{\infty} (-1)^{n+1} E_n (n\pi/1-\xi) \right. \\ &\left. \times \exp\left(. - \frac{R_{\mathrm{B}} + (n\pi/1-\xi)^2}{Pe}\tilde{x}\right)\right). \end{aligned}$$

Eq. (18) is solved numerically for each $\tilde{x}$ location, yielding the loci of the reaction plane, $\xi(x)$, along the drop circumference.

3. Results

We now compare the results of the present study with those of the stagnant film model of Ramachandran and Sharma (1969) and their conditions:

$$D_{\mathrm{A}} = D_{\mathrm{B}} = 10^{-5}\ \mathrm{cm^2/s}, \quad C_{\mathrm{A}i} = 1\text{–}3 \times 10^{-5}\ \mathrm{g\ mol/cm^3}, \quad C_{\mathrm{BS}} = 3 \times 10^{-5}\ \mathrm{g\ mol/cm^3},$$
$$k_{\mathrm{s}} = 1\text{–}2 \times 10^{-3}\ \mathrm{cm/s}, \quad k_{\mathrm{l}} = 2\text{–}5 \times 10^{-3}\ \mathrm{cm/s}, \quad A_{\mathrm{p}} = 3000\ \mathrm{cm^2/cm^3}.$$

3.1. Location of the reaction plane

Typical drops in a spray absorber have diameter in the range of 1000–2000 μm. The falling velocity U of these drops is in the range of $U = 5$–10 m/s. Therefore, using the Hadamard and Rybczynski solution, we obtain

$$\frac{u}{U}=\frac{1}{1+\mu_{\mathrm{l}}/\mu_{\mathrm{g}}}\left(1-2\tilde{r}^{2}\right)\ \rightarrow\ u=5\text{–}10\ \mathrm{cm/s}. \tag{19}$$

For these conditions, the Peclet number is in the range of 1000–5000.

The location of the reaction plane is presented in Fig. 3 in terms of the dimensionless reaction plane location, as a function of the dimensionless distance along the drop circumference for different Peclet numbers. The case of $Pe=0$ solved by Ramachandran and Sharma (1969) is also presented for comparison.

We note that for the stagnant film solution of Ramachandran and Sharma (1969), $Pe=0$, the location of the reaction plane is constant and independent of the position on the drop. In the present solution the higher the Peclet number the larger the deviation from the stagnant film solution. We may, therefore, conclude that the convection terms in the mass balance equations cause a shift of the reaction plane towards the gas–liquid interface. This shift is more drastic as internal circulation increases, i.e., at high Peclet numbers. In particular, for conditions of our data, with Peclet number is in the range of 1000–5000 deviation from the stagnant flow solution is very significant. On the other hand, at lower Peclet numbers, say $Pe<100$, the reaction plane locus approaches the stagnant film reaction plane already after a 'short' distance from the drop pole. Therefore, for these conditions the problem may be treated using the stagnant film solution of Ramachandran and Sharma.

3.2. Local mass transfer rate

From the solution for the reaction plane loci, the local mass transfer rate, $\hat{\mathbf{N}}_{\mathbf{A}}$, is obtained in the following way:

$$\hat{\mathbf{N}}_{\mathbf{A}}=-D_{\mathrm{A}}\frac{\partial C_{A}}{\partial y}\bigg|_{y=0}=-\frac{D_{\mathrm{A}}C_{\mathrm{A}i}}{\delta}\frac{\partial\tilde{C}_{\mathrm{A}}}{\partial\tilde{y}}\bigg|_{\tilde{y}=0}, \tag{20}$$

and substituting δ from Eq. (11) we obtain.

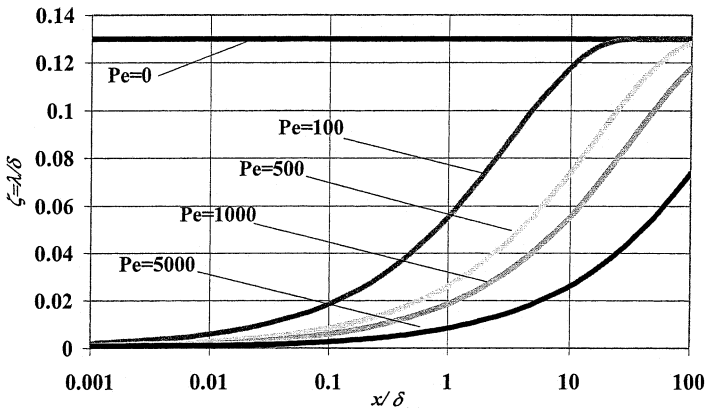

Fig. 3. Reaction plane loci vs dimensionless distance from stagnation region for various Peclet numbers.

$$\hat{\mathbf{N}}_{\mathbf{A}} = k_{\mathrm{l}} C_{\mathrm{A}i} \left.\frac{\partial C_{\mathrm{A}}}{\partial y}\right|_{y=0} = \mathbf{N}_{\mathbf{A}} \left.\frac{\partial \tilde{C}_{\mathrm{A}}}{\partial \tilde{y}}\right|_{\tilde{y}=0}. \tag{21}$$

The dimensionless mass transfer rate is defined as,

$$\tilde{\mathbf{N}}_{\mathbf{A}} = \frac{\hat{\mathbf{N}}_{\mathbf{A}}}{\mathbf{N}_{\mathbf{A}}} = -\left.\frac{\partial \tilde{C}_{\mathrm{A}}}{\partial \tilde{y}}\right|_{\tilde{y}=0} = Sh_{\delta}(\tilde{x}), \tag{22}$$

where the Sherwood number may be rewritten with the help of Eq. (11) as

$$Sh_{\delta} = \frac{\hat{k}_{\mathrm{l}}\delta}{D} = \frac{\hat{k}_{\mathrm{l}}}{k_{\mathrm{l}}}. \tag{23}$$

Here k_{l} and $\mathbf{N}_{\mathbf{A}}$ are respectively the liquid side mass transfer coefficient and local mass transfer rate, both without solids dissolution, chemical reaction and liquid convection. The mass transfer coefficient and local mass transfer rate that account for these phenomena are $\hat{k}_{\mathrm{l}}$ and $\hat{\mathbf{N}}_{\mathbf{A}}$, respectively. Viewing Eqs. (22) and (23) one notes that the dimensionless mass transfer rate represented by the Sherwood number denotes the local enhancement in mass transfer relative to that without liquid convection, solids dissolution and chemical reaction.

Fig. 4 shows the dimensionless local mass transfer along the drop perimeter, calculated for different Peclet numbers.

Here again, the convection inside the liquid film enhances the local mass transfer rate as compared to that of the stagnant film model. By analyzing the local mass transfer results, it is clear that internal circulation enhances gas absorption.

3.3. Overall mass transfer rate

The calculation scheme of the overall mass transfer begins with a specific drop diameter d_{p}, and velocity U. The lateral velocity u inside the drop near the gas–liquid interface is determined using

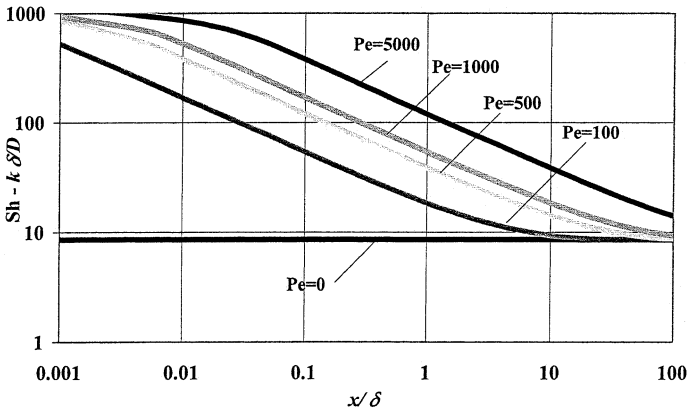

Fig. 4. Local mass transfer rate vs dimensionless distance from stagnation region for various Peclet numbers.

Eq. (19). The Peclet number is defined by the characteristic velocity u and the characteristic length δ. The regions in which the stagnant film model can be applied, and the region in which the present model has to be used is defined by means of Eq. (32) in Appendix A. The location of the reaction plane in each region is found by solving numerically Eq. (18). This equation is solved by trial and error for any given $\tilde{x}$ along the drop surface, while the local mass transfer rate is obtained from Eq. (20). In the final step the overall mass transfer rate is calculated by numerical integration of the local mass transfer along the drop surface, using Eq. (24).

$$\tilde{M}_{\mathrm{A}} = \int Sh(x)\,\mathrm{d}s = \frac{\hat{M}_{\mathrm{A}}}{M_{\mathrm{A}}} = \phi, \tag{24}$$

where $\hat{M}_{\mathrm{A}}$ is the overall mass transfer rate using the present model, and M_{A} is the overall mass transfer rate in the absence of chemical reaction, solid dissolution and convection. As a result, the overall dimensionless mass transfer rate represents the absorption enhancement due to these effects.For our two-region model, Eq. (24) is rewritten as

$$\tilde{M}_{\mathrm{A}} = 2\left(\int_0^{x1} \tilde{\mathbf{N}}_{\mathrm{A}}\,\mathrm{d}x + \int_{x1}^{x2} \tilde{\mathbf{N}}_{\mathbf{A}}\,\mathrm{d}x + \int_{x2}^{x3} \tilde{\mathbf{N}}_{\mathbf{A}}\,\mathrm{d}x \right). \tag{25}$$

The local mass transfer in region 1, of Fig. 2, is calculated using the one-dimensional model of Ramachandran and Sharma, $Pe = 0$, while that in region 2 is calculated by the present model, which accounts for convection.

The dimensionless overall mass transfer data, representing the overall enhancement factor, are shown in Fig. 5, in terms of absorption enhancement relative to that without chemical reaction and convection. From Fig. 5 we conclude that absorption enhancement exceeds that in a stagnant drop when $Pe > 100$. At lower Peclet numbers, i.e., at lower circulating rates, the reaction plane loci rapidly approach those calculated under the assumption of a stagnant drop, as shown in Fig. 3. Hence, for this case the contribution of internal circulation may be neglected.

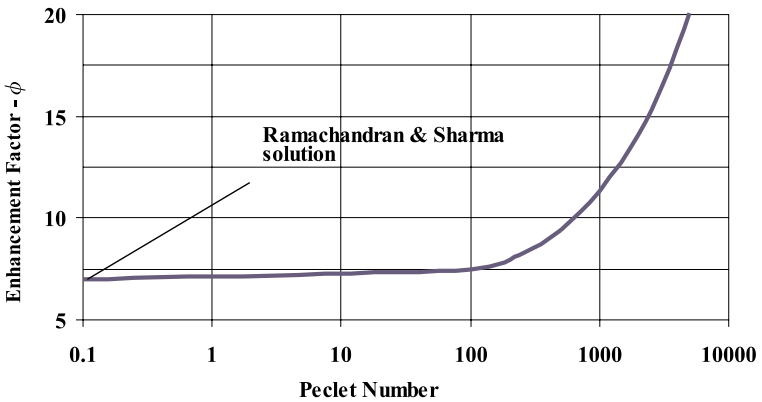

Fig. 5. Overall enhancement factor vs Peclet number.

3.4. Parametric investigation

The effect of particle specific area, A_p, and its solubility, i.e., saturation concentration, C_{BS}, on the absorption rate at different Peclet numbers were investigated.

Particle specific area, A_p, is the surface area of the particles per unit volume of liquid, and is given by

$$A_p = \frac{6W}{\rho_s d_s}, \tag{26}$$

where W is the solids weight concentration in the slurry, ρ_s their density and d_s the particle average diameter. For example, in absorption of acidic gas with a lime/limestone slurry

$$W = 0.1\text{–}0.2 \text{ g solids/cm}^3 \text{ slurry}, \quad d_s = 10^{-4}\text{–}3 \times 10^{-4} \text{ cm}, \quad \rho_s = 2 \text{ g/cm}^3,$$

and therefore,

$$A_p = 1000\text{–}6000 \text{ cm}^2/\text{cm}^3.$$

The solubility is also related to particle size, amount of turbulence in the liquid and chemical composition of the liquid. In gas absorption systems, the solids solubility is $\sim 10^{-5}$ g mol/cm^3. The solubility may be drastically increased with addition of weak carbonic acids to the slurry. The results of this investigation are shown in Figs. 6 and 7.

From these figures, we conclude that at high circulation rates, say $Pe > 3000$, increasing the solid specific area or the solubility of the solids has little practical benefit.

4. Comparison with experimental data

The results of the present investigation were compared with the experimental results of Sada et al. (1977), who studied SO_2 and CO_2 absorption into $Ca(OH)_2$ slurry, using a well-stirred tank as well as with the stagnant film model.

From the data in Sada et al. (1977), we estimate the average liquid velocity for a stirring at 100 rpm and tank radius of 5 cm as

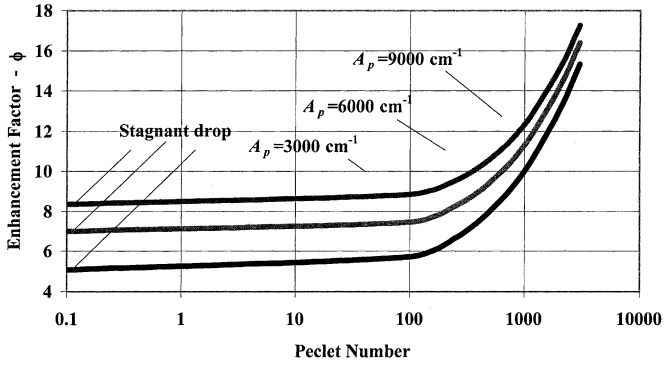

Fig. 6. Overall enhancement factor vs Peclet number at different specific solids area.

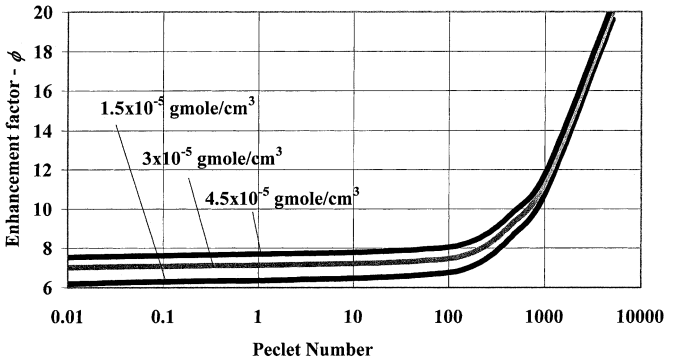

Fig. 7. Overall enhancement factor vs Peclet number for various solubility values of the solids.

$$u = \frac{\int_0^r \omega r 2\pi r \, \mathrm{d}r}{\pi r^2} = \frac{2}{3}\omega r = \frac{2\pi}{3} \times \frac{100}{60} \times 5 \cong 17.5 \text{ cm/s}, \tag{27}$$

where ω (s^{-1}) is the stirring frequency, and r (cm) is the tank radius.

The Peclet number in the stirred tank was estimated using u in Eq. (27) as the characteristic velocity, and δ in Eq. (11) as the characteristic length

$$Pe = \frac{u\delta}{D} = \frac{u}{k_l} = \frac{17.5}{0.005} \approx 3500. \tag{28}$$

Fig. 8 shows the enhancement in absorption rate relative to that into a saturated liquid without suspended solids and without convection, for the present model, that of the stagnant-film, and the experiments of Sada. The enhancement factor is defined as

$$\phi' = \frac{\hat{M}}{M'}, \tag{29}$$

where M' is the overall mass transfer without solids dissolution and without convection.

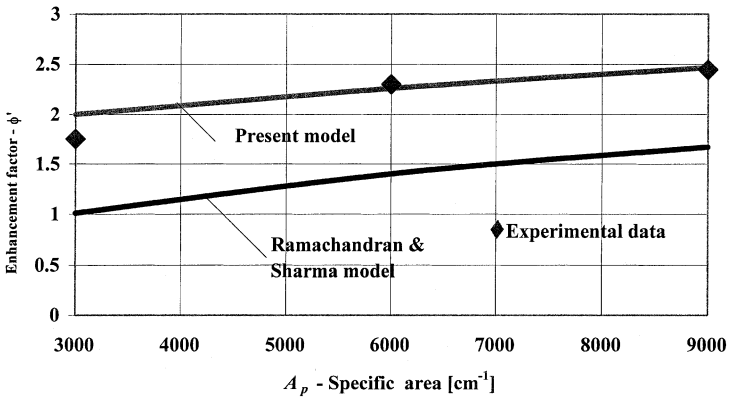

Fig. 8. Experimental and theoretical enhancement factors as a function of solids specific area.

The figure shows that the stagnant-film model underestimates the actual absorption rate, while the present model fits the experimental data quite well.

The fact that the liquid drop constitutes in the present model the disperse phase, while in the experimental data the disperse phase is comprised of gas bubbles has no effect on the validity of the comparison. In both cases, the absorbed gas dissolves and diffuses into a thin liquid film, where it reacts with the dissolved solids. Therefore, in both cases it is the flow inside the liquid film near the gas–liquid interface that affects the absorption rate.

5. Discussion and conclusions

Comparing absorption rates of the present model, with the experimental data from the literature, and with those of the stagnant-film model, we conclude:

- The effect of convection in the liquid film is to cause a shift of the reaction plane towards the gas–liquid interface, resulting in an increased local mass transfer rate.
- The present model does not take into account the convection of suspended solids from the drop core to the gas–liquid interface during absorption. For long absorption times, this may affect the validity of the calculated results, which are based on the assumption of a constant amount of suspended solids inside the liquid film. At long absorption times, this assumption is not valid any more, due to solids depletion.
- Figs. 4 and 5 indicates that the influence of internal circulation on the absorption rate cannot be neglected when $Pe > 100$.
- From Figs. 5–8 it is clear that the 'stagnant-film' model underestimates the absorption rate. Hence, we may conclude that liquid circulation, which exists near the gas–liquid interface, enhances the absorption rate.
- Gas absorption may be enhanced by increasing the solids specific area by grinding or increasing the solids concentration in the slurry, or by adding a weak organic acid that buffers the pH and increases the alkalinity in the scrubbing liquid (Rochelle and King, 1977). These activities affect strongly the overall cost of the scrubbing system. Therefore, it is essential to carefully assess the real benefit of such activities. From our analysis, see Figs. 6–8, we note that at high Peclet numbers, say $Pe > 3000$, there is little benefit in increasing either the particle specific area or the solubility. At high Peclet numbers, the convection of the soluble gas near the gas–liquid interface is the dominant factor in absorption. Wellek et al. (1970) and Brogren and Karlsson (1997) came to similar conclusions in their works.
- More research is required in order to obtain an accurate estimate of the degree of circulation inside a drop with suspended solids, and the changes in the circulation with time as the drop travels along the scrubber.
- In the present model, only instantaneous reactions were considered, although it is well known that in flue gas desulfurization (FGD) processes based on limestone or lime, some of the reaction rates may be finite. The present model may be modified to account for finite rate reactions, such as those considered by Brogren and Karlsson (1997) and Bronnikowska and Dudzinski (1991). By doing this, more accurate results may be obtained.

Acknowledgements

This research was supported by the Fund for Promotion of Research at Technion – Israel Institute of Technology.

Appendix A

We assume that the liquid velocity in regions 1 is small as compared to region 2. This assumption holds when the velocity ratio β is

$$\beta = \left|\left(\frac{v_r}{v_\theta}\right)\right|_{r \to a} \approx \left|\left(\frac{v_y}{v_x}\right)\right|_{y \to 0} \ll 1. \tag{30}$$

Substitution of the velocities from the Hadamard and Rybczynski solution yields,

$$\beta = \frac{1 - r^2}{1 - 2r^2} \cot\theta.$$

Substituting $y = 1 - r$

$$\beta_{y \to 0} \cong \frac{2y}{4y - 1} \cot\theta. \tag{31}$$

Near the gas–liquid interface we substitute $y \cong \delta$, therefore the limits of the stagnant region are obtained by solving the following inequality:

$$\beta = \frac{2\delta}{4\delta - 1} \cot\theta \ll 1. \tag{32}$$

A.1. Numerical example

For $D_A = D_B = 10^{-5}$ cm^2/s, $k_l = 0.002$ cm/s, the numerical value of δ is found from Eq. (11) as $\delta = 0.005$ cm. For $d_p = 0.1$ cm and $\beta < 0.1$ the stagnant region as calculated from Eq. (32) is confined to $0 < \theta < 6°$, $174° < \theta < 180°$, the corresponding numerical values of the arc length $\tilde{x}$, as shown in Fig. 2 are $\tilde{x}_1 = 0.8$, $\tilde{x}_2 = 31.2$, $\tilde{x}_3 = 32$.

From this numerical example, we conclude that the stagnant region holds about 7% of the total drop circumference. Hence, it is much shorter than the convection region.

Trying values of β between 0 and 0.2 it was found that the overall mass transfer rate is not affected strongly by the choice of β. The results here refer to $\beta = 0.1$.

References

Bjerle, I., Bengtsson, B., Färnkvist, K., 1972. Absorption of SO_2 in $CaCO_3$ slurry in laminar jet absorber. Chem. Eng. Sci. 27, 1853–1861.

Brogren, C., Karlsson, H.T., 1997. Modeling the absorption of SO_2 in a spray scrubber using the penetration theory. Chem. Eng. Sci. 52, 3085–3099.

Bronnikowska, W.P., Dudzinski, K.J., 1991. Absorption of SO_2 into aqueous systems. Chem. Eng. Sci. 46, 2281–2291.

Danckwerts, P.V., 1970. Gas–Liquid Reactions. McGraw-Hill, NewYork.
Hadamard, J., 1911. Mouvement permanent lent d'une sphere liquid et visqueuse dans un liquid visqueux. Compt. Rend. 152, 1735.
Handlos, A.E., Baron, T., 1957. Mass and heat transfer from drops in liquid–liquid extraction. Am. Institute Chem. Eng. J. 3, 127–136.
Happel, J., Brenner, H., 1965. Low Reynolds Number Hydrodynamics. Prentice-Hall, Englewood Cliffs, NJ.
LeClair, B.P., Hamielec, A.E., Pruppacher, H.R., Hall, W.D., 1972. A theoretical and experimental study of the internal circulation in water drops falling at terminal velocity. J. Atmos. Sci. 29, 728–740.
Levich, V.G., 1962. Physicochemical Hydrodynamics. Prentice-Hall, New York.
Mehra, A., 1996. Gas absorption in reactive slurries: particle dissolution near gas–liquid interface. Chem. Eng. Sci. 51, 461–477.
Ramachandran, P.A., Sharma, M.M., 1969. Absorption with fast reaction in a slurry containing sparingly soluble fine particles. Chem. Eng. Sci. 24, 1681–1686.
Rochelle, G.T., King, C.D., 1977. The effect of additives on mass transfer in $CaCO_3$ or CaO slurry scrubbing of SO_2 from waste gases. Industrial Eng. Chem. Fundam. 16, 67–75.
Rybczynski, W., 1911. Uker die Fortschreitende Bewegung einer fluessigen Kugel in einem zaehen Medium. Bull. Acad. Cracovie. Ser. A 40–60.
Sada, E., Kumazawa, H., Butt, M.A., 1977. Single gas absorption with reaction in slurry containing fine particles. Chem. Eng. Sci. 32, 1165–1170.
Sherwood, T.K., Pigford, R.L., Wilke, C.R., 1975. Mass Transfer. McGraw-Hill, New York.
Uchida, S., Koide, K., Shindo, M., 1975. Gas absorption with fast reaction into slurry containing fine particles. Chem. Eng. Sci. 30, 644–646.
Ukawa, N., Takashina, T., Shinoda, N., Shimizu, T., 1993. Effects of particle size distribution on limestone dissolution in wet FGD process applications. Environ. Progress 12, 123–131.
Watada, H., Hemielec, A.E., Johnson, A.I., 1970. A theoretical study of mass transfer with chemical reaction in drops. Can. J. Chem. Eng. 48, 225–261.
Wellek, R.M., Anode, W.V., Brunson, R.J., 1970. Mass transfer with chemical reaction inside droplets and gas bubbles: mathematical mechanisms. Can. J. Chem. Eng. 48, 645–655.
Wyllie, C.R., 1995. Advanced Engineering Mathematics, sixth ed. McGraw-Hill, New York.